38th International Electric Vehicle Symposium and Exhibition (EVS38) Göteborg, Sweden, June 15-18, 2025

Composite Battery Module with Integrated Tab Cooling System

Leonard John[1], Simon Dillmann[2], Lars-Fredrik Berg[2], Jens Tübke[3], Martin Doppelbauer[4]
[1]*Fraunhofer ICT, leonard.john@ict.fraunhofer.de (corresponding author),*
[2] *Fraunhofer ICT*
[3] *Fraunhofer ICT and Institute of Mechanical Process Engineering and Mechanics (MVM), Karlsruhe Institute of Technology (KIT),*
[4] *Institute of Electrical Engineering (ETI), Karlsruhe Institute of Technology (KIT) and Fraunhofer ICT*

Executive Summary

This paper presents the conception, design, prototyping, and thermal investigation of a Composite Battery Module featuring an Integrated Tab Cooling System. Aimed at improving thermal management in pouch-type lithium-ion battery cells, various potential cooling strategies were discussed on their respective advantages and limitations for the integration in composite housings.

A significant advancement is the design of the Integrated Connection and Cooling Plate (ICCP). It enhances industrial applicability of battery cell tab cooling. Effective thermal coupling is ensured through a composite plastic overmolding that provides electrical isolation and simplifies assembly processes.

A full prototype was fabricated to assess manufacturability, cooling performance, and resistance to thermal runaway. The heat transfer through the cell terminal was investigated and the considerable impact on the overall cooling confirmed. Thermal evaluation of the complete module is performed on the testbench and supported by simulation.

Keywords: Batteries; Thermal Management; Battery Manufacturing; Packaging, Cooling & Heat Transfer

1 Introduction and cooling concepts

In the initial phase of conceptualizing the Composite Battery Module, a comprehensive analysis of pouch-type battery cells was conducted. These cells are typically characterized by three distinct outer surfaces, forming a basic six-sided prism: one or two terminal sides with tabs, seam sides, and flat sides.

Each of these surfaces presents various cooling approaches, which possess unique advantages and disadvantages, as outlined in Table 1. In conventional metal-based battery housings, the cool plate concept for seam-side cooling of pouch cells is widely adopted due to its straightforward design.

Terminal or tab cooling offers the potential for an additional cooling location, which can enhance cooling power and achieve a more uniform temperature distribution [13, 14]. This improved thermal management may contribute to slower aging of the battery cells [14, 15]. However, existing terminal cooling designs commonly require significant bending of the tabs [7, 8], complicating industrialization efforts.

In the design of automotive battery housing there is a clear trend toward composite structures, due to the promised benefits of the advantages of material properties (e.g. C-fiber reinforced or fire-resistant composites) and reduced costs (reduced part numbers, design for mass production) [16–18].

While there are clear advantages for the tab cooling outlined, in the research field of composite battery casings the cooling concepts still focus on the known seam side cell cooling via a cooling plate. This can be produced as a hybrid aluminum-plastic part [11] and integrated in the battery tray bottom [12] as depicted in Figure 1a. Consequently, this study on composite battery design seeks to address the challenge of developing a more streamlined tab cooling solution by utilizing advanced plastic manufacturing techniques.

Table 1: Cooling Concepts on different cell faces

		Flat side cooling	Seam side cooling	Terminal cooling
Cooling properties	pro	most surface area for a good thermal connection	Depending on the internal structure of the cell, an equal cooling over all active layers can be expected. Also, there is more cooling area than on the terminals	Cooling the tab allows equal cooling of all cell-layers, as each current collector is electrical and thermal equally connected to the tab
	con	The heat flux is orientated orthogonal to the current collectors, thus higher resistance and unequal cooling between the layers. Cooling takes a lot of space	The thermal resistance through the pouch bag can be quite high, especially if the seam is uneven and not adjacent to the active layers. The thermal interface needs to be flexible to adjust for cell expansions	The thermal resistance can be high because of long paths and thin and small tabs itself
Existing Concepts and solutions		Industrial and research solutions: Conductive plates used by Chevrolet [1] Heat pipe systems [2] Microchannel cold plates [3, 4]	Seam side cooling became the industry standard for pouch cell cooling e.g.: VW ID.3 batterie [5] Hyundai Ioniq 5 [6]	Research paper concepts: Cool plate on top of the welded tab weld seam [7] Tabs clamped to a cooling pipe [8] Heat conductive material connecting the tab with the side cool plate [9]
Composite plastic hosing concepts		Potential concepts include plastic plates embedded with PCM materials [10] or microchannels. These plates could further integrate fire protection and cell swelling properties.	Metal plastic hybrid cooling plates as part of the Battery tray, similar to the solutions presented in [11, 12]	

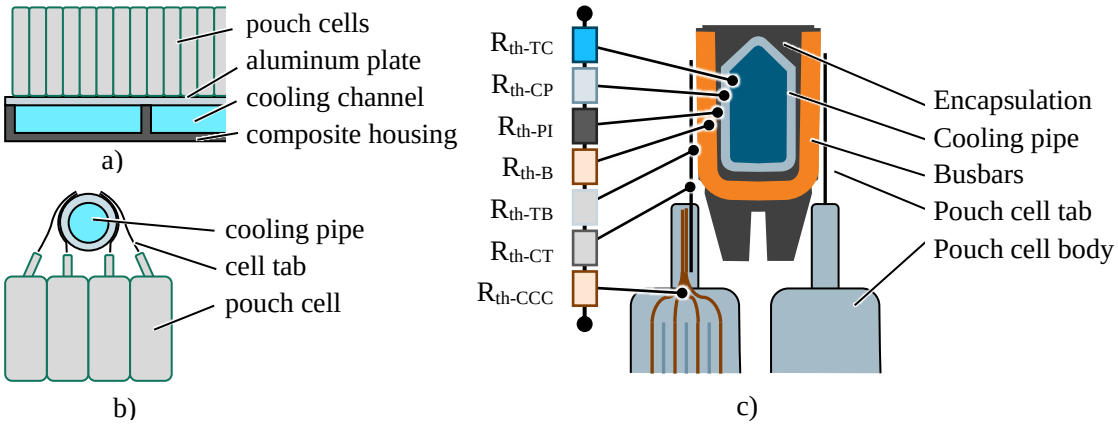

Figure 1: Cooling concepts for a Composite Battery: a) Hybrid cool plate similar to [11,12]; b) concepted tab cooling as presented in [8]; c) Presented concept with encapsulated busbar around a cooling pipe

2 Design of the Integrated Connection and Cooling Plate

The presented cooling structure improves upon the cooling pipe based design introduced by Liebertseder [8] (visualized in Figure 1b). Additional busbars are incorporated between the cooling pipe and the battery cell tab. The cooling pipe is constructed from aluminum, ensuring water proofness and facilitating easier industrialization with bent profiles. For the prototype, an additive manufactured pipe solution was targeted, while a bend pipe solution would be more interesting in a large scale production.

To ensure mechanical integrity, the busbars and the cooling pipe are overmolded. The composite plastic used for the overmolding serves multiple functions. Firstly, it establishes a critical interface between the busbar and the cooling pipe, where electrical isolation is essential while maintaining effective thermal coupling. By optimizing the molding process, a plastic layer thickness of approximately 0.35 mm is sufficient for electrical isolation. Combined with the thermal conductivity of 0.9 W/(m·K) of the Sumikon® EME-G720E epoxy-based composite, a heat transfer coefficient of 2570 W/(m²·K) is achieved. Furthermore, the plastic overmold consolidates around 28 components including busbars, isolation, cooling pipe, and BMS-sensor cable into a single part, creating the Integrated Connection and Cooling Plate (ICCP). As a combined part it reduces risks associated with the assembly of the module.

A demonstration battery module has been designed using 24 counter-tab pouch cells stacked face-to-face, connected in a 1p24s configuration (Figure 2). The cooling channel is routed in a meandering path between the busbars. The positioning of the tabs on the cells leads to a module design featuring two opposing ICCPs.

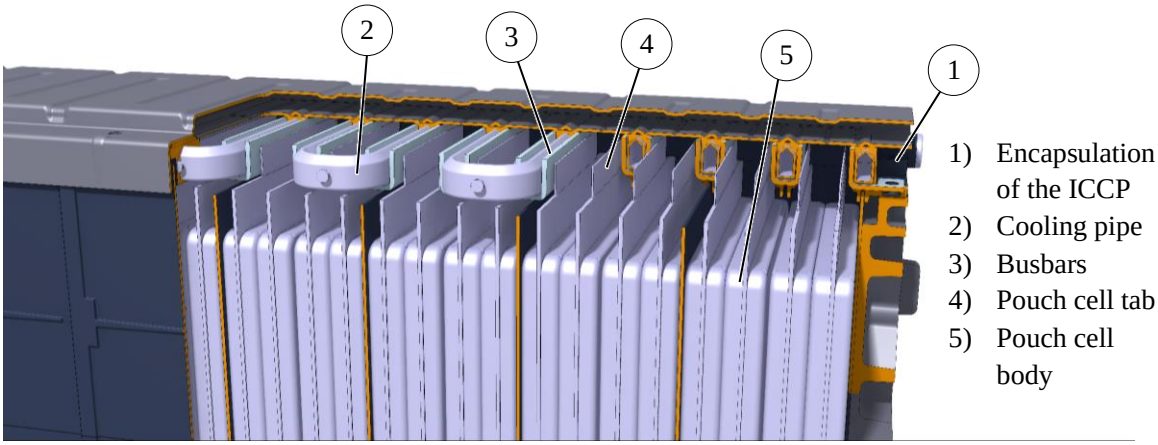

Figure 2: Design of the Integrated Connection and Cooling Plate (ICCP): 3D rendering view of the partially cut composite battery module

3 Prototype fabrication

To investigate manufacturability, cooling behavior, and resistance to thermal runaway, a full prototype of the Composite Battery Module was constructed. The ICCP was produced through several steps: fabrication of the inserts, assembly of the inserts, overmolding, and finishing.

3.1 Inserts

The busbars are fabricated from aluminum ENAW6060. Additionally, a flexible flat cable for battery management system (BMS) voltage measurement is integrated and welded to the busbars. For the prototype, the cooling pipe is manufactured from aluminum using the Laser Powder Bed Fusion (LPBF) process. To support the thin walls of the pipe, the enclosed powder is removed only after overmolding, following the method outlined in [19]. This approach ensures that the powder provides internal support for the thin walls and prevents the cooling pipe from being filled with plastic. The cooling pipe is wrapped at several locations with fiberglass tape to ensure the correct positioning of the busbars. The assembled Inserts (Figure 3) are ready to be placed into the mold for the encapsulation

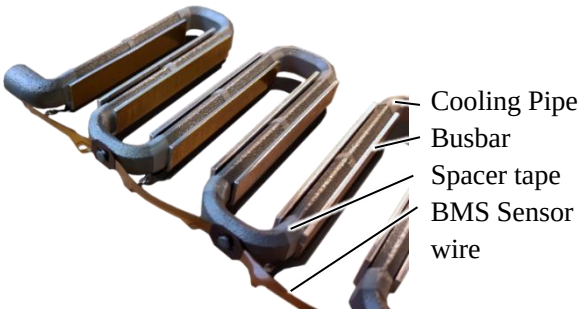

Figure 3: Assembled ICCP Inserts

3.2 Encapsulation

The encapsulation is performed using a transfer molding process with Sumikon® EME-G720E (Figure 4a). The thin isolation areas were fully filled; however, complete electrical isolation between the busbars and the cooling pipe was not always achieved. This limitation is primarily due to the manually bent busbars and slightly thicker cooling pipes. A cross-section of the fabricated ICCP is shown in Figure 4b, where the insulation layer thickness is measured to range from 0.2 to 0.3 mm (compared to the CAD design of 0.35 mm), while the cooling pipe wall thickness is slightly greater than the planned 0.7 mm, measuring between 0.77 and 0.85 mm.

3.3 Finishing

After the molding process, any potential plastic flash is removed. The ends of the cooling pipe are then drilled open to allow for the removal of aluminum powder from inside the pipe. Figure 4a shows an almost finished ICCP (The pipe inlet is missing the cutting of the threads).

4 Investigation of terminal heat transfer

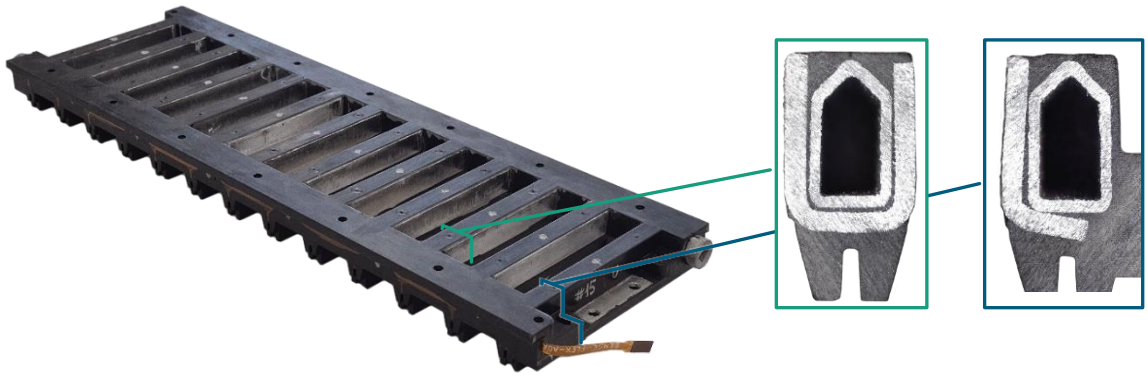

a) b)

Figure 4: a) Overmolded ICCP, b) Cut view through busbars with cooling channel. Left: Correct “U”-busbar; Right: Example for an isolation error (on last busbar)

For a tab cooled battery module, the heat transfer through the cell terminal, into the heatsink is of special significance for the overall cooling. A simple thermal resistor diagram analysis will bring insight into the thermal behavior in this region. Table points out that the thermal resistance in the short tab is at least an order higher than the other materials the heat has to pass through. Around 57 percent of the heat resistance are due to the tab. So, it is obvious that the cell manufacturer has great influence on the tab cooling properties. Using a double thick and fifty percent wider copper tab would reduce the total thermal resistance by 60 percent.

In a tab-cooled battery module, the heat transfer through the cell terminal into the heatsink is critically important for the overall cooling performance.

The heat transfer from the tab to the busbar is heavily influenced by the contacting method employed. Both spot welding and laser welding techniques have been tested; however, the experimental battery is constructed with clamped tabs to maintain a degree of flexibility for potential disassembly.

To determine the heat transfer coefficient in clamped tabs, a small test setup was established (see Figure 5). A nickel sheet simulates the tab and is clamped onto thermoelectric elements using brackets and thermally conductive paste. The thermoelectric elements actively transfer heat through the nickel tab, resulting in a temperature differential of 55 K across the 64 mm long sheet with a cut area of 6 mm². In contrast, only a temperature difference of approximately 2.5 K was observed between the 180 mm² tab contacting area and the surface of the piezoelectric element. This suggests a favorable heat transfer coefficient of approximately 800 W/(m²·K), although measurements obtained via thermal imaging may introduce significant uncertainties.

A simplified thermal resistor network analysis provides valuable insights into the thermal behavior within this region. The in-line network analysis in Table 2 (represented in Figure 2a) indicates that thermal resistance within the counts for over 50 percent of the total thermal resistance. Ther heat transfer through the clamped tab contributes another 25 percent. Thus, it is evident that the choice of materials and design by the cell manufacturer significantly affects the tab's cooling efficiency. Increasing the thickness and width of the copper tab by 50 percent could potentially reduce the total thermal resistance by up to 60 percent.

Table 2: Heat transfer through the cell terminal

Thermal resistor as depicted in Figure 2b	Material	λ /(W/m K)	α /(W/m²K)	A /mm²	l /mm	R_{th} /(K/W)
$R_{th\text{-}TC}$: Transfer into coolant	-	-	450	775	-	2.87
$R_{th\text{-}CP}$: Cooling pipe wall	EN AC 43000	160	-	775	0.7	0.006
$R_{th\text{-}PI}$: Plastic isolation	EME-G720E	0,9	-	775	0.35	0.50
$R_{th\text{-}B}$: Busbar	EN AW 6060	210	-	775	1.5	0.009
$R_{th\text{-}TB}$: Transfer into Busbar	-	-	800	168	-	7.44
$R_{th\text{-}CT}$: Cell Tab	Nickel	69	-	8.4	9	15.53
$R_{th\text{-}CCC}$: Cell current collectors	Aluminum	210	-	57.3	9	0.75
$R_{th\text{-}T}$: Terminal total						27.10

λ: Thermal conductivity; α: Heat transfer coefficient; A: Cross sectional area; l: Length;
R_{th}: Thermal resistance

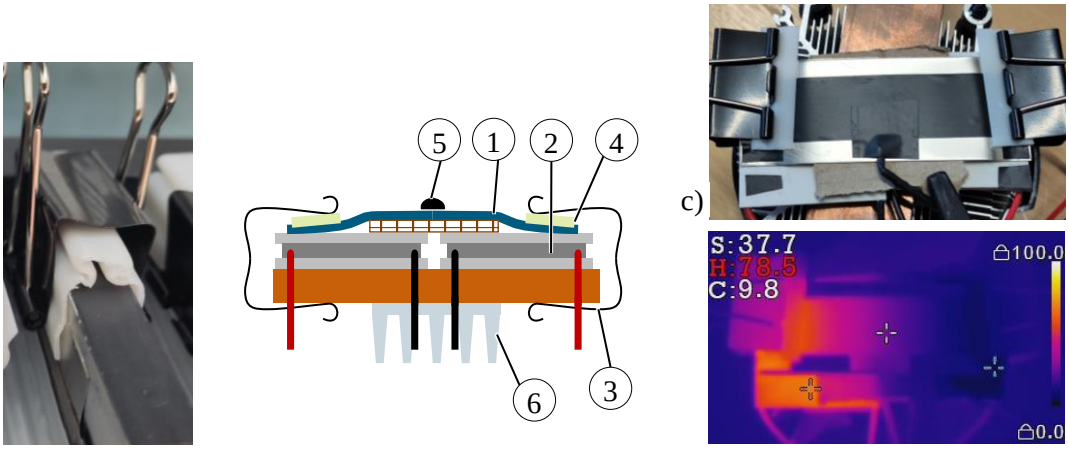

Figure 5: Heat through tab analysis. a) Tab clamped at the module; b) Derived Testbench with 1: Nickle sheet, 2: Peletier element, 3: Foldback clip, 4: Isolation, 5: Reference temperature sensor, 6: Heat sink; c) Test setup (black tape as measuring surface); d) Thermal picture

5 Thermal investigation of the full module

5.1 Test stand

To gain insight into the thermal behavior of the composite battery housing, a module consisting of 24 66 Ah LCO cells was assembled. For the thermal investigation, every second cell is equipped with a temperature sensor. Additionally, three cells are fitted with an array of sensors to determine potential gradients within the cells. The cooling system supplies the module with a water-glycol solution at a flow rate of 2.5 l/min and is equipped with thermal probes, as well as volumetric flow and pressure sensors. Both integrated cooling circuit paths (ICCPs) are connected in series for cooling. The experimental chamber maintains an average temperature of 22 °C, and the module is not further thermally insulated. Figure 6 shows the testbench module on a rack placed over an emergency water bath.

Figure 6: Battery module on the testbench. White cables for additional BMS Sensing, copper wires for thermocouples.

5.2 Simulation

A three-dimensional thermal transient simulation was conducted using FEM software. The half cells are composed of the active cell body, the current collector merging area, the tab welding area, and the tab. The first two areas exhibit anisotropic thermal conductivity for modeling their thermal behavior. The terminal properties of every other cell vary, representing the different current collectors materials copper and aluminum. The tab itself is represented as pure nickel sheet material.

5.3 Passive cooling

Using a C/2 discharge, the module was heated to approximately 45 °C cell temperature with the cooling system turned off. Thermal imaging reveals that the ICCPs are much warmer than the cells, reaching temperatures up to 60 °C. This observation confirms the initial assumption regarding the

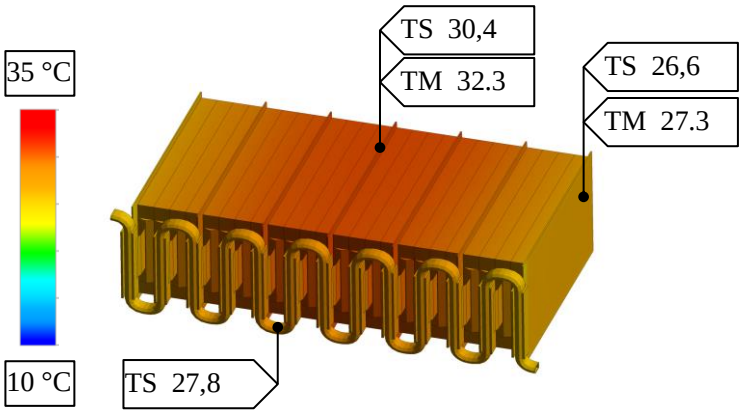

Figure 7 Simulated heat distribution after 2h passive cooling. TS: Simulated temperature point, TM: Measured temperature point

necessity of tab cooling to maintain optimal operating temperatures. Without further electrical operation or cooling, the module is allowed to cool passively. After 2 hours, it cools solely through radiation and free convection at the outer surfaces, achieving a maximum cell temperature of 32 °C. The simulation of this cooling process yields comparable results (see end distribution in Figure 7), confirming the analytically estimated heat transfer coefficient of 5 W/(m²K).

5.4 Active cooling

After the module is reheated to 45 °C cell temperature through an unchilled C/2 discharge (down to an average cell voltage of 3.04 V). With the water-glycol liquid cooling system activated at a flow rate of 2.5 l/min with a 0.4 bar pressure drop over both ICCPs, the module cools down to 23 °C within 2 hours as shown in Figure 8.

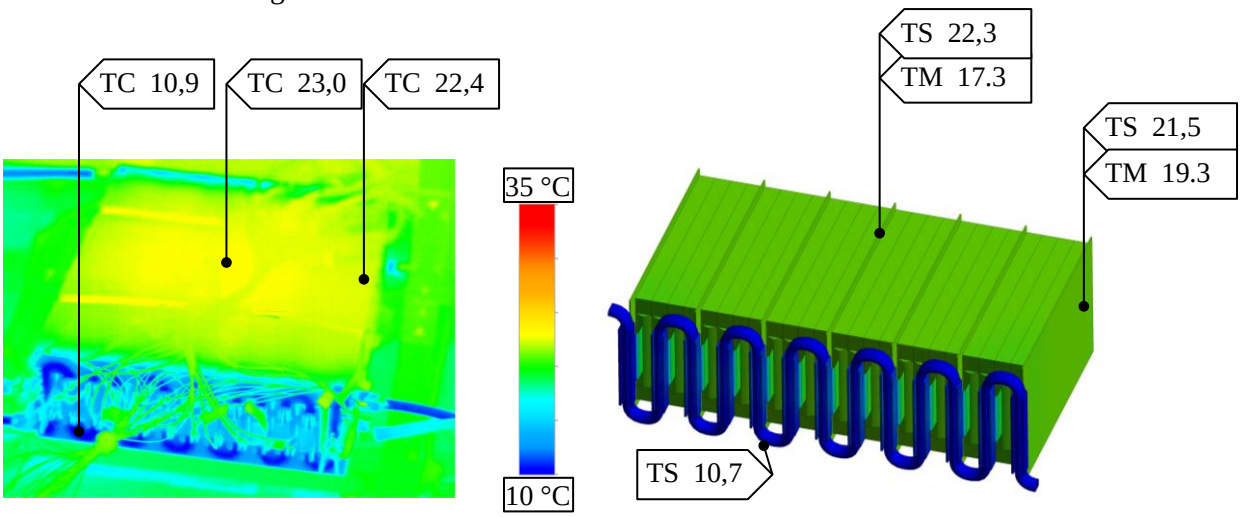

Figure 8: Temperature distribution after 2h active cooling. Left: thermal picture with camera-based Temperature measurements (TC); Right: Simulated reference view with simulated (TS) and measured (TM) Temperature data points. Point data in °C

5.5 Discussion of basic thermal investigations

The simulations and experiments discussed in the preceding chapters are interpreted to determine the thermal behavior of a composite battery module featuring an integrated tab cooling system. In addition to assessing temperature distribution, it is essential to establish simplified thermal resistance values. In a basic linear network model, the battery dissipates heat via a thermal resistance to the environment and another thermal resistance associated with the cooling system. These resistance values are intended to facilitate extrapolation to other applications.

Findings from the uncooled cooling experiment suggest that the thermal resistance value to the environment is $R_{th\text{-}Environment}$ = 0.7 W/K. In the actively cooled cooling experiment, both the cooling to the environment and the internal cooling systems interact, albeit at different cooling temperatures. The thermal resistance value to the cooling system can be derived from the accompanying equivalent circuit diagram, yielding a value of $R_{th\text{-}Cooling\text{-}System}$ = 1.1 K/W.

The cooling resistance across the active Cell material up to the Tab ends (up to $R_{th\text{-}CT}$ as outlined in Table 2) is determined via simulation to $R_{th\text{-}Cell}$ = 7.89 K/W, which corresponds to a CCC_{Tabs} value of 0.127 W/K according to [20]. It is noteworthy that an increase of 1 mm in tab length results in an increase of 1.37 K/W in thermal resistance. It can be concluded that the thermal resistance of the ICCP per cell is $R_{th\text{-}ICCP\_cell}$ = 18.51 K/W.

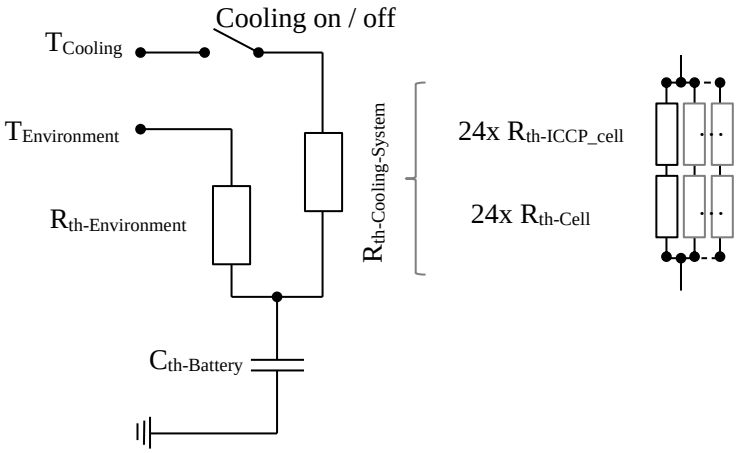

Figure 9: Basic thermal cooling network of the module

5.6 **Module with enhanced cell terminals**

As discussed in chapter 4, a significant limitation of the terminal cooling strategy is the high thermal resistance of the cell tabs. The simulation of the module allows the evaluation of the performance when incorporating enhanced cell designs. Therefore, the simulation model has been modified to include cells with the following changed specifications: The use of copper and aluminum tab materials (former nickel), an increased tab width of 66 mm (up from 42 mm), and a greater tab thickness of 0.5 mm (compared to the previous 0.125 mm). These modifications not only decrease thermal resistance but also expand the heat transfer surface area between the tab and busbar, while simultaneously lowering the electrical resistance, thereby reducing the resultant Joule heating. Due to these changes the steady state temperature of a simulated module under constant heat generation can be reduced by 66 percent, confirming the pure analytical results of chapter 4.

5.7 Charging C/2 and cell temperature distribution

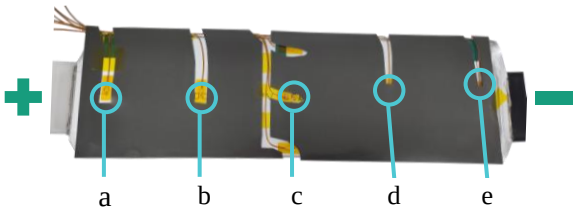

Figure 11: Mounting position of thermocouples on pouch cells. Slots in the compression pad prevent indentation

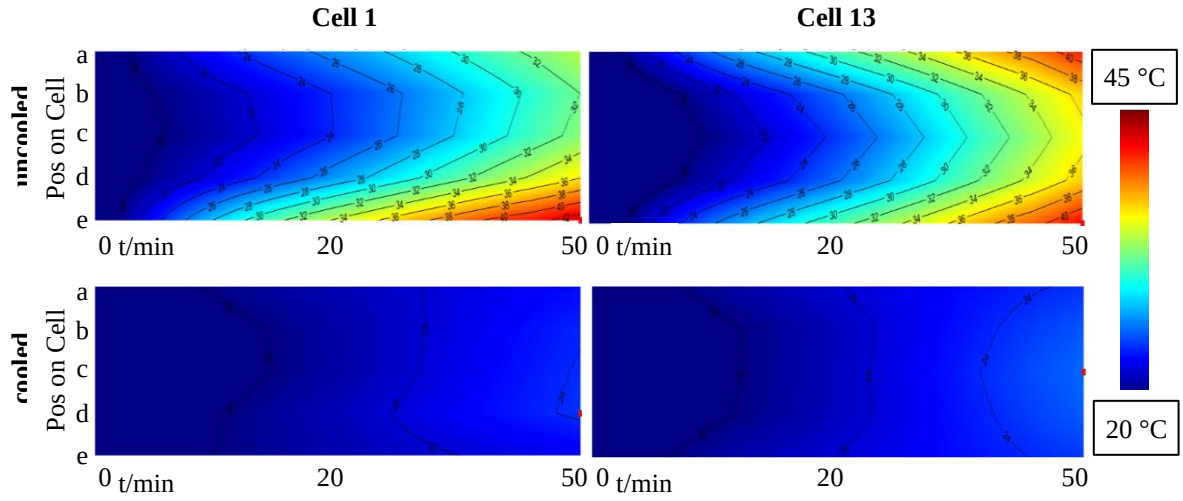

Figure 10: Temperature distribution over time on Cell 1 and 13. Upper: uncooled; Lower: cooled

To assess the thermal performance of the Integrated Tab Cooling system, three battery cells within the module were instrumented with surface-mounted thermocouples. The positioning of the sensors followed the configuration shown in Figure 11, with thermocouples placed at locations a through e along the longitudinal axis of each cell. During the experiments, the module was subjected to a charging current corresponding to a C-rate of C/2 over a time span of 50 minutes. Temperature data from the thermocouples were continuously recorded and are presented in time-resolved plots. A color scale is used to indicate the measured temperature levels at the sensor positions. All measurements were conducted under ambient temperature conditions. The first row of the results illustrates the temperature distribution in the uncooled reference configuration during charging. The second row depicts the thermal response of the cell when the Integrated Tab Cooling system is active under identical charging conditions. The cooling system operated with a volumetric flow rate of 2.5 L/min using a 50% / 50% water-glycol mixture as coolant, and a coolant temperature of 10 °C.

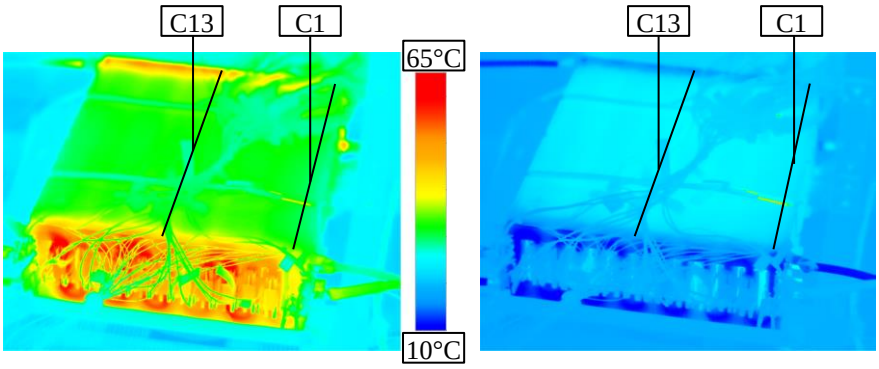

Figure 12: Thermal vision on the module after 50 min charging with (right) and without cooling (left). Position of the cells 1 and 13 are marked

The initial temperature of cell 1 was 20 °C. After 50 minutes of charging at a rate of 0.5C, the maximum recorded cell temperature of the uncooled test was 42.95 °C, measured at sensor position e. As illustrated in Figure 10 (upper left) the cell exhibits an asymmetric temperature distribution along the cell. Specifically, one tab reaches a temperature of approximately 32 °C, while the opposing tab exhibits a significantly higher temperature of around 43 °C. The asymmetry on cell 1 ban be explained by the cooling effect the charging cable: As illustrated in Figure 12 is located directly at the one battery module terminal. Additional the clamped electrical connection as used on this research module can be found as a source of varying contact resistance. This may lead to higher local heat generation. The experiment conducted with the actively cooled battery module demonstrates a significantly more homogeneous temperature distribution across the cell surface (Figure 10 lower left). After 50 minutes of charging at 0.5C, the maximum temperature recorded was 24.23 °C.

In the uncooled configuration, Cell 13 (right in the graphs) – positioned centrally within the module – exhibited an initial temperature of 20 °C, reaching a maximum of 41.77 °C at measuring point e after 50 minutes of charging at 0.5C. The temperature distribution along both measurement points close to the cell tabs was largely symmetric over the cell, in contrast to the previously observed asymmetry on cell 1.

Under active tab cooling, the temperature levels at the tab-adjacent measurement points closely matched those in the center of the cell. The maximum temperature recorded in this configuration was 25.61 °C.

These results demonstrate that the integrated tab cooling system not only reduces the overall temperature rise during operation but also promotes a more uniform thermal distribution across the cell.

5.8 **Discharging 1.0 C and cell temperature distribution**

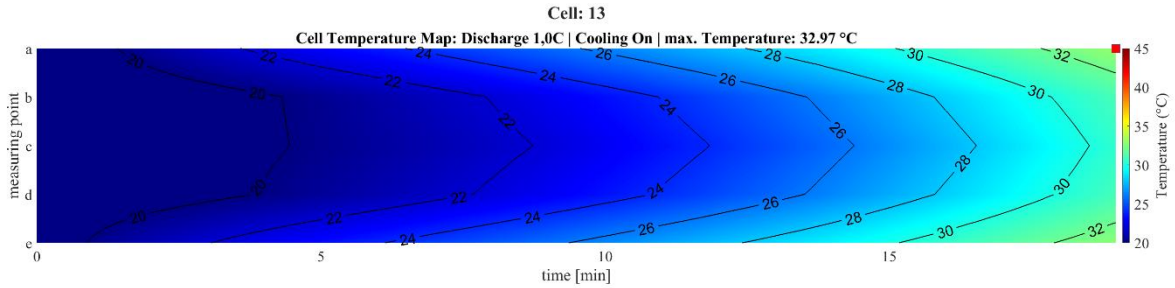

Figure 13: Temperature distribution over time on Cell 13 during a 1,0C Discharge

In order to further test the tab cooling, an investigation was conducted under increased current load, corresponding to a discharge rate of 1.0 C. The volumetric flow rate of the coolant was maintained at 2.5 L/min. The coolant temperature was set to 10 °C, while the initial cell temperatures were 20 °C. As a representative example, cell 13 – positioned at the center of the module – is examined. Compared to the conditions shown in Figure 10 (lower right), this cell exhibits a noticeably higher temperature increase caused by the higher current. The maximum temperature was recorded in the vicinity of the cell tab and reached 32.97 °C. The total discharge duration was approximately 19 minutes and had to be terminated due to one cell reaching 2,8 V which is the end-of-discharge voltage of the used cell.

6 Summary and Outlook

6.1 Summary

This paper presents a thorough examination of a Composite Battery Module equipped with an Integrated Tab Cooling System, designed to enhance thermal management for pouch-type lithium-ion batteries. The authors discuss various cooling strategies, highlighting the advantages and limitations of each method for integration into composite housings. A key feature is the Integrated Connection and Cooling Plate (ICCP), which facilitates industrial applicability by ensuring effective thermal coupling while providing electrical isolation through a composite plastic overmold.

Prototype development was undertaken to evaluate manufacturability, cooling performance, and resistance to thermal runaway. Significant findings include the identification of thermal resistance issues associated with the cell tabs. The study also demonstrates the importance of optimizing tab design, suggesting that increasing tab thickness and width can substantially reduce thermal resistance.

Thermal evaluations conducted on a test bench, alongside simulation studies, confirm the effectiveness of the ICCP in maintaining optimal operating temperatures within the battery module. In basic heat dissipation tests, the overall and cooling specific thermal resistance was identified

In a charging cycles it was shown how the Tab cooling does not only impact the cell temperature, but also improves a uniform temperature distribution over the cell.

6.2 Outlook

Future work should focus on refining the design and manufacturing processes of the ICCP to further enhance thermal connection with the cell. With focus on testing, higher charge and discharge rates are necessary to evaluate the performance of the presented tab cooling.

7 Acknowledgments

We would like to express our gratitude to Sumitomo Bakelite Europe (Genth) NV for commissioning this research project. We thank them for the successful collaboration and for granting us the opportunity to publish these results freely. We also like to acknowledge the support received from the framework KAMO Karlsruhe Mobility High Performance Center (www.kamo.one), the association of Karlsruhe's institutions for research, education, and transfer in the field of innovative mobility and logistics solutions.

8 References

[1] Sgraham. "Chevy Bolt EV Battery Disassembly and Charging Limitations." Accessed: Apr. 11, 2025. [Online]. Available: https://allev.info/2023/12/chevy-bolt-ev-battery-disassembly/

[2] D. M. Weragoda, G. Tian, A. Burkitbayev, K.-H. Lo, and T. Zhang, "A comprehensive review on heat pipe based battery thermal management systems," *Applied Thermal Engineering*, vol. 224, p. 120070, 2023, doi: 10.1016/j.applthermaleng.2023.120070.

[3] C. Lan, J. Xu, Y. Qiao, and Y. Ma, "Thermal management for high power lithium-ion battery by minichannel aluminum tubes," *Applied Thermal Engineering*, vol. 101, pp. 284–292, 2016, doi: 10.1016/j.applthermaleng.2016.02.070.

[4] Kausthubharam, P. K. Koorata, and S. Panchal, "Thermal management of large-sized LiFePO4 pouch cell using simplified mini-channel cold plates," *Applied Thermal Engineering*, vol. 234, p. 121286, 2023, doi: 10.1016/j.applthermaleng.2023.121286.

[5] N. Wassiliadis *et al.*, "Quantifying the state of the art of electric powertrains in battery electric vehicles: Range, efficiency, and lifetime from component to system level of the Volkswagen ID.3," *eTransportation*, vol. 12, p. 100167, 2022, doi: 10.1016/j.etran.2022.100167.

[6] J. AYTES and A. Di Nunno, *Hyundai Ioniq 5: Integrated cooling plate | Battery Pack Breakdown.*

Accessed: Apr. 11, 2025. [Online]. Available: https://www.youtube.com/watch?v=5PASNQU5RSw
[7] H. Heimes, A. Kampker, A. Mohsseni, F. Maltoni, and J. Biederbeck, "Cell Tab Cooling System for Battery Life Extension," in *2019 18th IEEE Intersociety Conference on Thermal and Thermomechanical Phenomena in Electronic Systems (ITherm)*, Las Vegas, NV, USA, 2019, pp. 1125–1133, doi: 10.1109/ITHERM.2019.8757444.
[8] J. Liebertseder, A. Dollinger, T. Sorg, L.-F. Berg, and J. Tubke, "Battery Tab Cooling in Traction Battery Modules using Thermally Conductive Plastics," in *2022 IEEE Vehicle Power and Propulsion Conference (VPPC)*, Merced, CA, USA, 112022, pp. 1–5, doi: 10.1109/VPPC55846.2022.10003372.
[9] S. H. Ham, D. S. Jang, M. Lee, Y. Jang, and Y. Kim, "Effective thermal management of pouch-type lithium-ion batteries using tab-cooling method involving highly conductive ceramics," *Applied Thermal Engineering*, vol. 220, p. 119790, 2023, doi: 10.1016/j.applthermaleng.2022.119790.
[10] W. Wu, W. Wu, and S. Wang, "Thermal optimization of composite PCM based large-format lithium-ion battery modules under extreme operating conditions," *Energy Conversion and Management*, vol. 153, pp. 22–33, 2017, doi: 10.1016/j.enconman.2017.09.068.
[11] Sogefi. "Hybrid cold plate." [Online]. Available: https://airandcooling.com/product/hybrid-cold-plate-batteries-component/
[12] T. Prucha, *Keep Your Cool: Electric Vehicle Battery Cooling Methods.* Accessed: Apr. 11, 2025. [Online]. Available: https://www.youtube.com/watch?v=9DNe4gi7NYs&t=1951s
[13] J. Liebertseder, "Thermal design optimization of traction battery modules using meta-model-based simulations," *Wissenschaftliche Schriftenreihe des Fraunhofer ICT; 99*, 2024, doi: 10.24406/publica-3308.
[14] I. A. Hunt, Y. Zhao, Y. Patel, and J. Offer, "Surface Cooling Causes Accelerated Degradation Compared to Tab Cooling for Lithium-Ion Pouch Cells," *J. Electrochem. Soc.*, vol. 163, no. 9, A1846-A1852, 2016, doi: 10.1149/2.0361609jes.
[15] L. Cloos and T. Wetzel, "In-Plane versus Through-Plane Thermal Gradients during Cyclic Aging of Lithium-Ion Batteries: An Experimental Study," *Energy Tech*, 2025, Art. no. 2402409, doi: 10.1002/ente.202402409.
[16] Ash, "The key enabler for powering the EV transition: lightweight composite battery enclosures | Mitsubishi Chemical Group," *Mitsubishi Chemical Group*, 29 Aug., 2024. Accessed: Apr. 26, 2025. [Online]. Available: https://automotive.mcgc.com/the-key-enabler-for-powering-the-ev-transition-lightweight-composite-battery-enclosures/
[17] "SGL Carbon produces prototypes of fully integrated composite battery enclosures for NIO's Advanced Technology." Accessed: Apr. 26, 2025. [Online]. Available: https://www.sglcarbon.com/en/newsroom/news/press-report/nio-battery-enclosure/
[18] Automotive Manufacturing Solutions. "Carbon composite footprint." Accessed: Apr. 26, 2025. [Online]. Available: https://www.automotivemanufacturingsolutions.com/materials/carbon-composite-footprint/39121.article
[19] L. John, D. Becker, S. Reuter, H.-C. Möhring, M. Doppelbauer, and L. F. Berg, "Resource Efficient Manufacturing of Complex Cooling Structures," in *Advances in Automotive Production Technology – Towards Software-Defined Manufacturing and Resilient Supply Chains* (ARENA2036), N. Kiefl, F. Wulle, C. Ackermann, and D. Holder, Eds., Cham: Springer International Publishing, 2023, pp. 307–313.
[20] A. Hales, L. B. Diaz, M. W. Marzook, Y. Zhao, Y. Patel, and G. Offer, "The Cell Cooling Coefficient: A Standard to Define Heat Rejection from Lithium-Ion Batteries," *J. Electrochem. Soc.*, vol. 166, no. 12, A2383-A2395, 2019, doi: 10.1149/2.0191912jes.

9 Presenter Biography

Leonard John graduated in mechanical engineering at the Karlsruhe Institute of Technology in 2022. Currently, he researches lightweight electrical motors and advanced battery housings at the Fraunhofer Institute for Chemical Technology ICT in Karlsruhe.